Electronic Supplementary Material (ESI) for ChemComm.

SUPPLEMENTARY INFORMATION

Descriptors of magnetic anisotropy revisited

Mauro Perfetti [1]* and Jesper Bendix [1,]*

[1] Department of Chemistry, University of Copenhagen, Universitetparken 5, 2100, Copenhagen, DK

***** Correspondence: mauro.perfetti@chem.ku.dk; bendix@kiku.dk

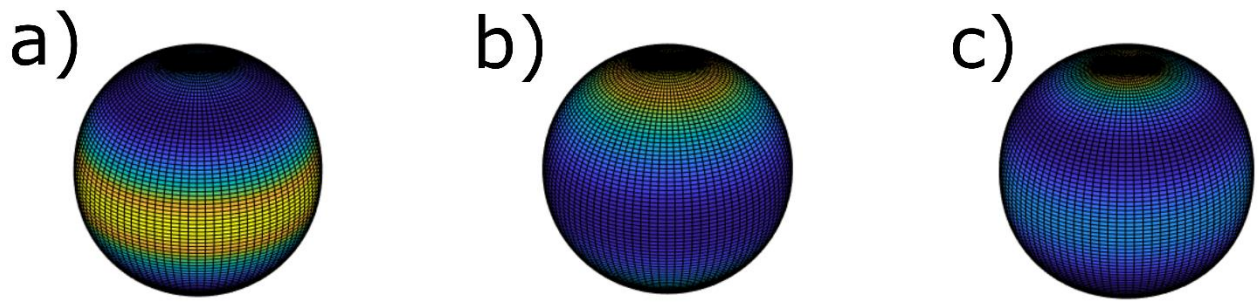

Figure S1. Free energy landscapes. a) easy axis, b) easy plane, c) easy cone. The color scale magnifies the intensity from low (deep blue) to high (orange). The simulations were obtained considering the CF parameters reported for the $HoPt_2$ complex (J = 8).[1] The EA landscape was obtained at B = 1 T and T = 2 K, the EP landscape at B = 1 T, T = 200 K and the EC landscape at B = 3 T and T = 18 K.

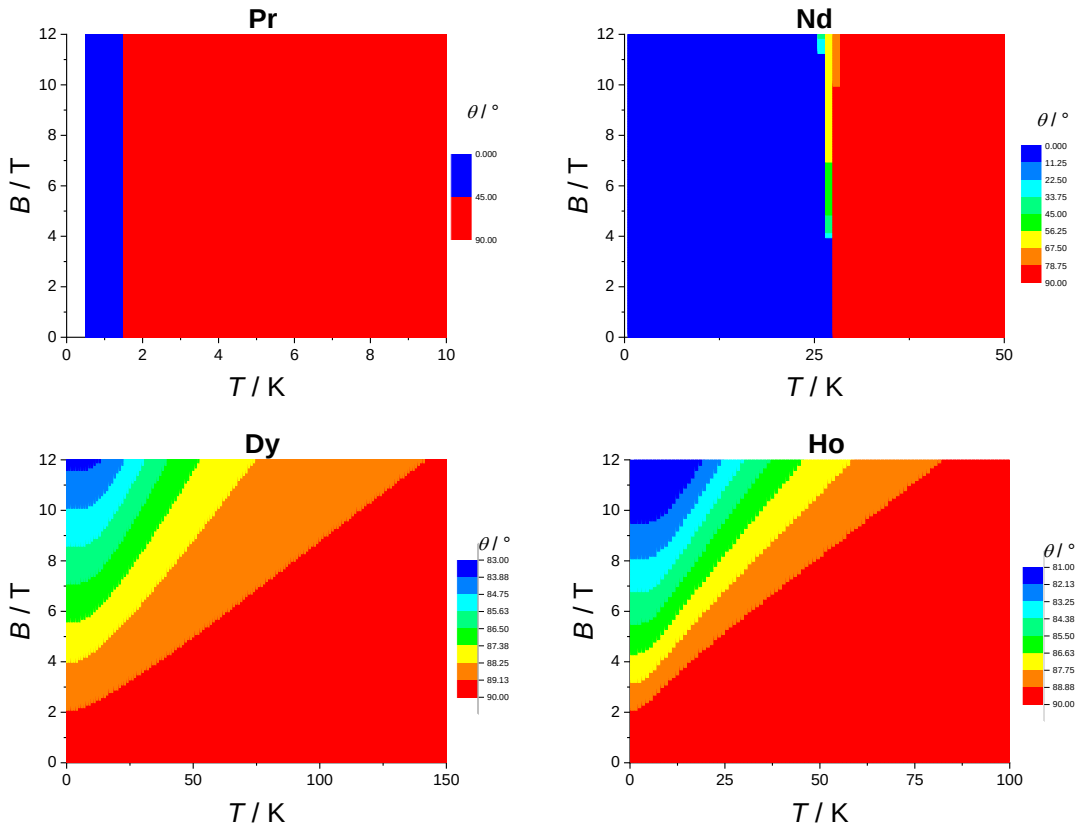

Figure S2. 2D magnetic anisotropy phase diagram for LnTRENSAL. Only derivatives exhibiting changes in the anisotropy are shown. CF parameters from ref. 2.

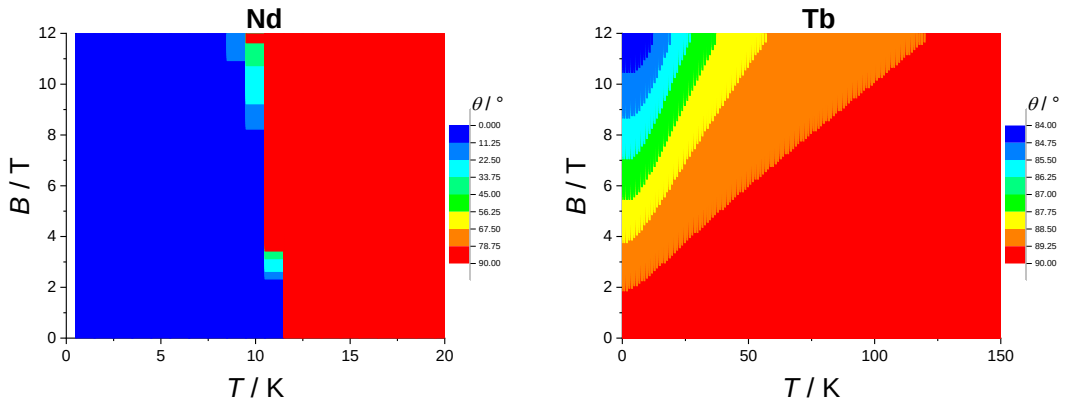

Figure S3. 2D magnetic anisotropy phase diagram for LnTRENOVAN. Only derivatives exhibiting changes in the anisotropy are shown. CF parameters from ref 3.

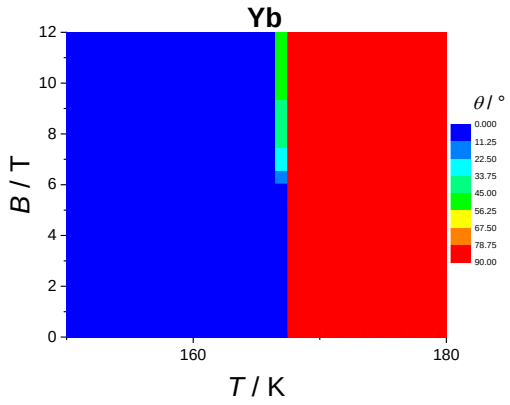

Figure S4. 2D magnetic anisotropy phase diagram for $LnPc_2$. Only derivatives exhibiting changes in the anisotropy are shown. CF parameters from ref 4.

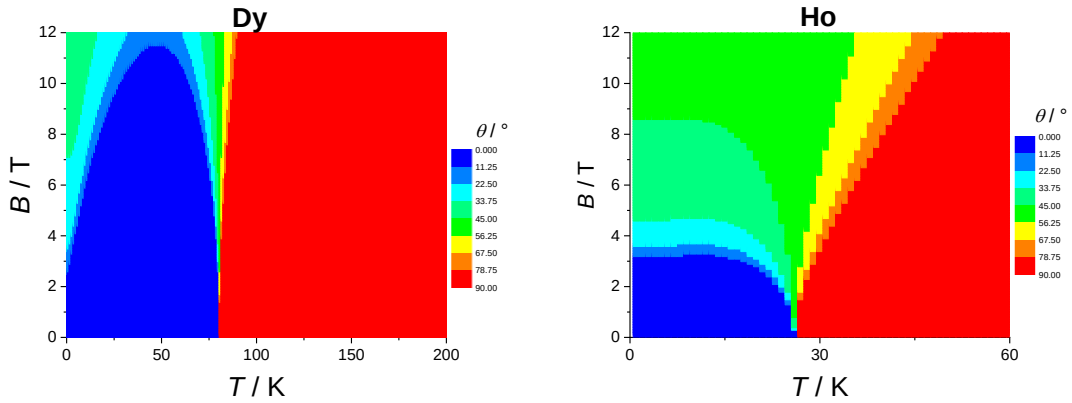

Figure S5. 2D magnetic anisotropy phase diagram for LnW_{10}. Only derivatives exhibiting changes in the anisotropy are shown. CF parameters from ref 5.

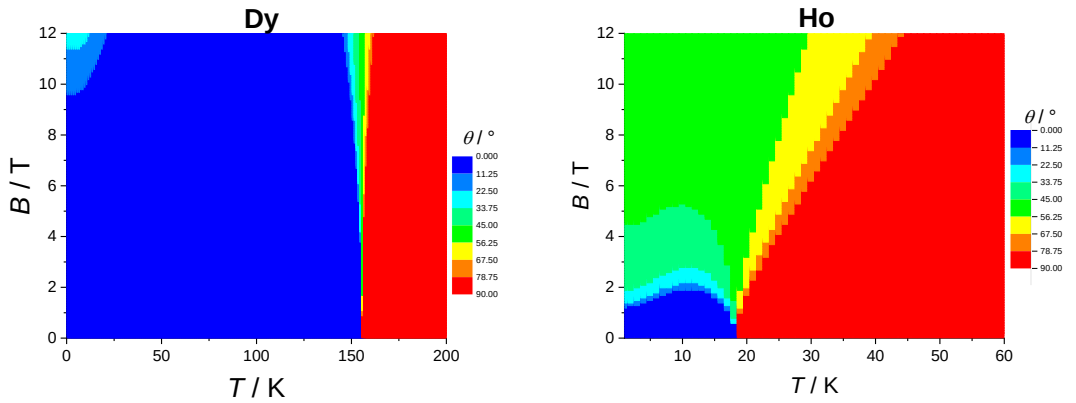

Figure S6. 2D magnetic anisotropy phase diagram for LnW_{22}. Only derivatives exhibiting changes in the anisotropy are shown. CF parameters from ref 5.

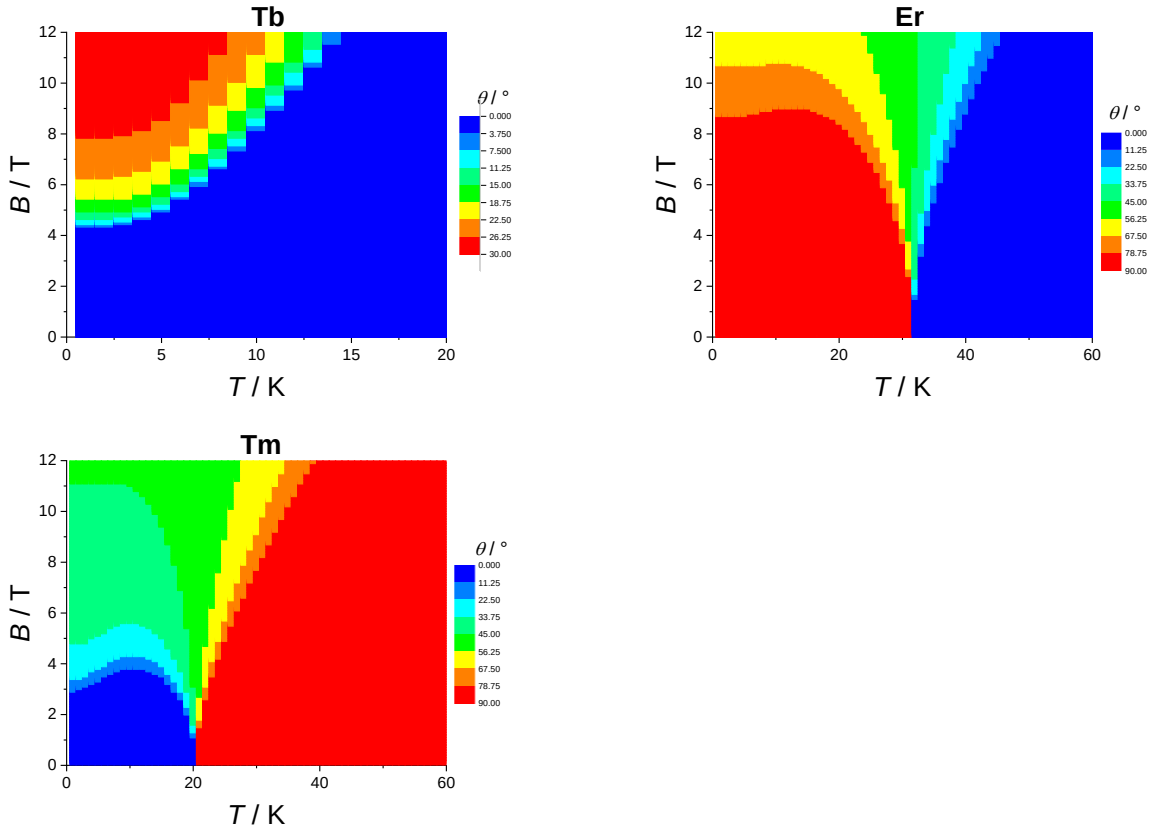

Figure S7. 2D magnetic anisotropy phase diagram for LnW_{30}. Only derivatives exhibiting changes in the anisotropy are shown. CF parameters from ref 6.

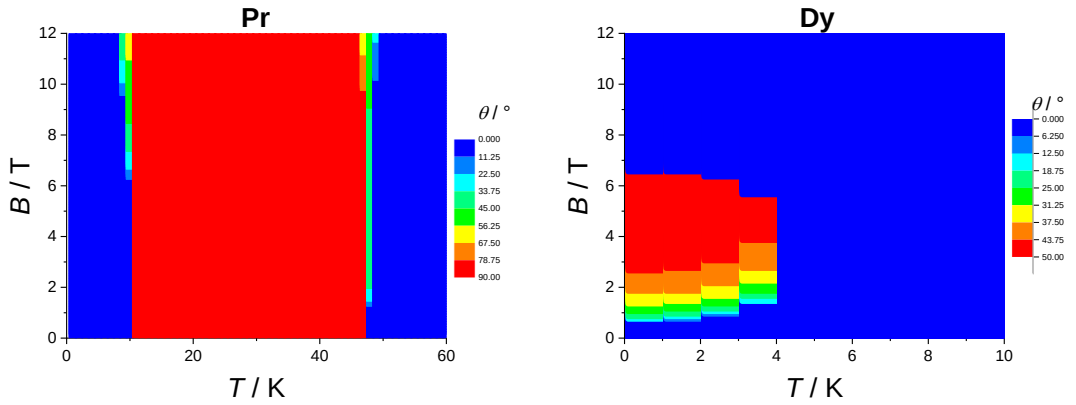

Figure S8. 2D magnetic anisotropy phase diagram for $LnCl_3$. Only derivatives exhibiting changes in the anisotropy are shown. CF parameters from ref 6. For Pr ref 7.

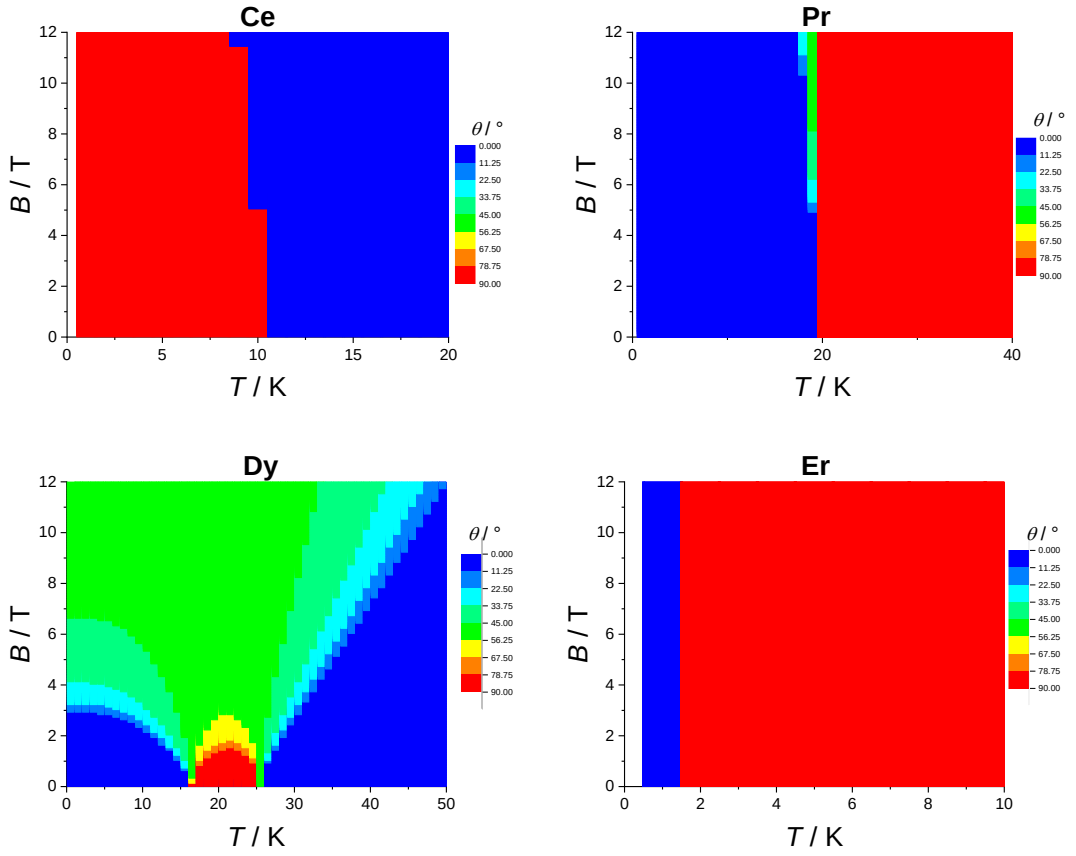

Figure S9. 2D magnetic anisotropy phase diagram for LnES. Only derivatives exhibiting changes in the anisotropy are shown. CF parameters from ref 6. For Dy ref 9. For Er ref 10.

Anisotropy switch: the energetic structure required.

Kramers ions. The Kramers theorem assures at least double degeneracy for half integer spins when the magnetic field is zero. In the ideal situation of pure doublets, all the states split when the magnetic field is applied along z, but only the |±1/2> doublet splits when the field is in the *xy* plane. Thus, especially at low fields, the |±1/2> contribution into a certain state is of paramount importance to determine if the anisotropy can be switched from EA to EP or *vice-versa*.

- Cerium. The $J = 5/2$ ground state of Ce^{3+} precludes the inclusion of sixth order terms in the CF potential, thus greatly simplifying the interpretation of the effect. The energy level diagram of CeES that has a ground pure |±1/2> state (EP) that is separated by 6.8 cm^{-1} from the |±5/2> (EA) excited state. As expected, CeES undergoes a complete (90°) and abrupt inversion (EP-EA) at ca. 10 K.

- Neodymium. NdTRENSAL and NdTRENOVAN exhibit an inversion EA-EP. In both cases the isolated ground doublet is primarily composed by $|\mp 5/2\rangle$ and $|\pm 1/2\rangle$, mixed by the off-diagonal CF parameters. At very low temperature the free energy along *z* is clearly lower than the one in *xy*, however when the thermal energy starts to be sufficient to populate both sublevels of the ground doublet, the free energy along *z* rapidly increases, while along *xy* it decreases due to the significant $|\pm 1/2\rangle$ component. NdTRENOVAN has a higher $|\pm 1/2\rangle$ percentage in the ground state compared to NdTRENSAL, resulting in an inversion occurring at lower temperature (ca. 10 K vs. 27 K).
- Erbium. The ground state of Er^{3+} is a $J = 15/2$, thus 8 doublets are expected in zero field. The two Er compounds that show inversion are $[PPh_4]ErPt_2$ and ErW_{30}. In both compounds, the fraction of $|\pm 1/2\rangle$ in the ground state is significant, while the first excited state is largely composed by $|\pm 13/2\rangle$, thus inversion (EP-EA) occurs at a temperature when the first excited state starts to be populated.
- Dysprosium. For Dy^{3+} the situation is more complicated, because inversion occurs at higher temperature ($T = 80 – 160$ K) compared to the other lanthanides, thus involving a larger number of levels. Four Dy compounds show inversion: DyW_{10}, DyW_{22}, $[PPh_4]DyPt_2$ and DyES. The case of DyES, that reverses anisotropy two times with temperature, is discussed in the main paper.
- Ytterbium. The only Yb^{3+} compound that was found to exhibit inversion is $YbPc_2$, that was modelled without inclusion of off-diagonal CF terms. The resultant picture is basically reversed compared to the CeES case, indeed when the ground $|\pm 5/2\rangle$ state is almost fully populated, the anisotropy is given by the first excited state (at ca. 160 K), that is a pure $|\pm 1/2\rangle$. The result is an abrupt inversion EP-EA at ca. 120K.

Non Kramers ions. The CF states of non Kramers ions in absence of a magnetic field can be singlets. This greatly complicates the rationalization of the anisotropy switch because the Zeeman diagrams are not easily predictable.

- Praseodymium. PrES and $PrCl_3$ exhibit a transition EA-EP at 20 K and 10 K, respectively. They both have a ground highly mixed pseudo-doublet (mainly $|\pm 4\rangle$ and $|\mp 2\rangle$) that leads to EA anisotropy at low temperature and EP anisotropy when sufficiently populated. However, the percentage of $|\pm 4\rangle$ state in the ground doublet is higher in $PrCl_3$ than in PrES (88% vs. 78%). This small difference is sufficient to promote a second anisotropy inversion for $PrCl_3$ at ca. 47 K, when the second excited state (the $|+3\rangle - |-3\rangle$ singlet) gets significantly populated.
- Holmium. The anisotropy inversion occurs in three Ho^{3+} compounds: HoW_{10}, HoW_{22} and $[PPh_4]HoPt_2$. The low-lying energy levels in all these molecules are essentially identical: a ground pseudo doublet mainly composed by $|\pm 4\rangle$ and a first excited state composed by $|\pm 5\rangle$. The ground pseudo doublet that has an effective *g* factor only slightly higher in the *z* direction than in the *xy* plane.[10] Thus, when temperature is raised, the EA anisotropy rapidly changes into EP anisotropy. Inversion temperatures are between 18 K and 27 K.
- Thulium. The only Tm^{3+} derivative that was found to possess a complete inversion is TmW_{30}. The energetic situation is similar to the case of Ho^{3+}, however in this case the two states involved in the transition (EA-EP) are the $|\pm 4\rangle$ (ground) and $|\pm 3\rangle$ (first excited). Transition temperature is ca. 20 K.

Synthesis and characterization of DyES

1.49 g of diethylsulfate (9.65 mmol, 20% more than the stoichiometric amount) were dissolved in 22 ml of water in the presence of 0.5 g (1.34 mmol) of Dy_2O_3. The mixture was kept in an oven at 80 °C for one day, followed by filtration and slow evaporation at room temperature. A single colourless crystal (mass: 326 μg) was extracted from the batch and indexed using Single Crystal diffractometer Xcalibur3 with a Mo source (Kα, λ = 0.71 Å). Xcalibur3 is a 4 cycles kappa geometry diffractometer equipped with a Sapphire 3 CCD detector.

Cantilever Torque Magnetometry

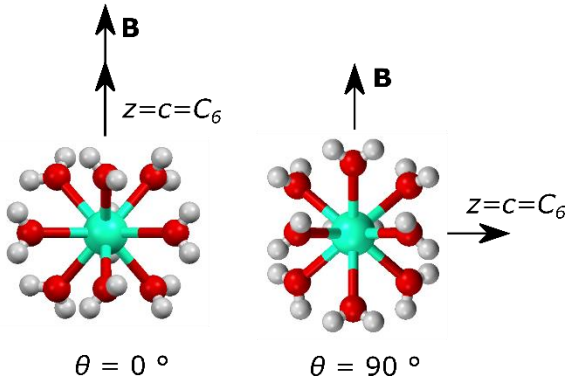

Figure S10. Orientation of the molecule during the rotation along the *a* crystallographic axis. Details about the experimental setup and the techniques can be found in literature [11]. The main magnetic axes (*xyz*) where imposed to be coincident with the orthogonal crystallographic axes (*ab'c*). This was justified by the small in-plane anisotropy (calculated to be 5 orders of magnitude smaller than the out of plane anisotropy). Colour code: Dy-cyan, O-red, H-white. The diamagnetic counterions were omitted for clarity.

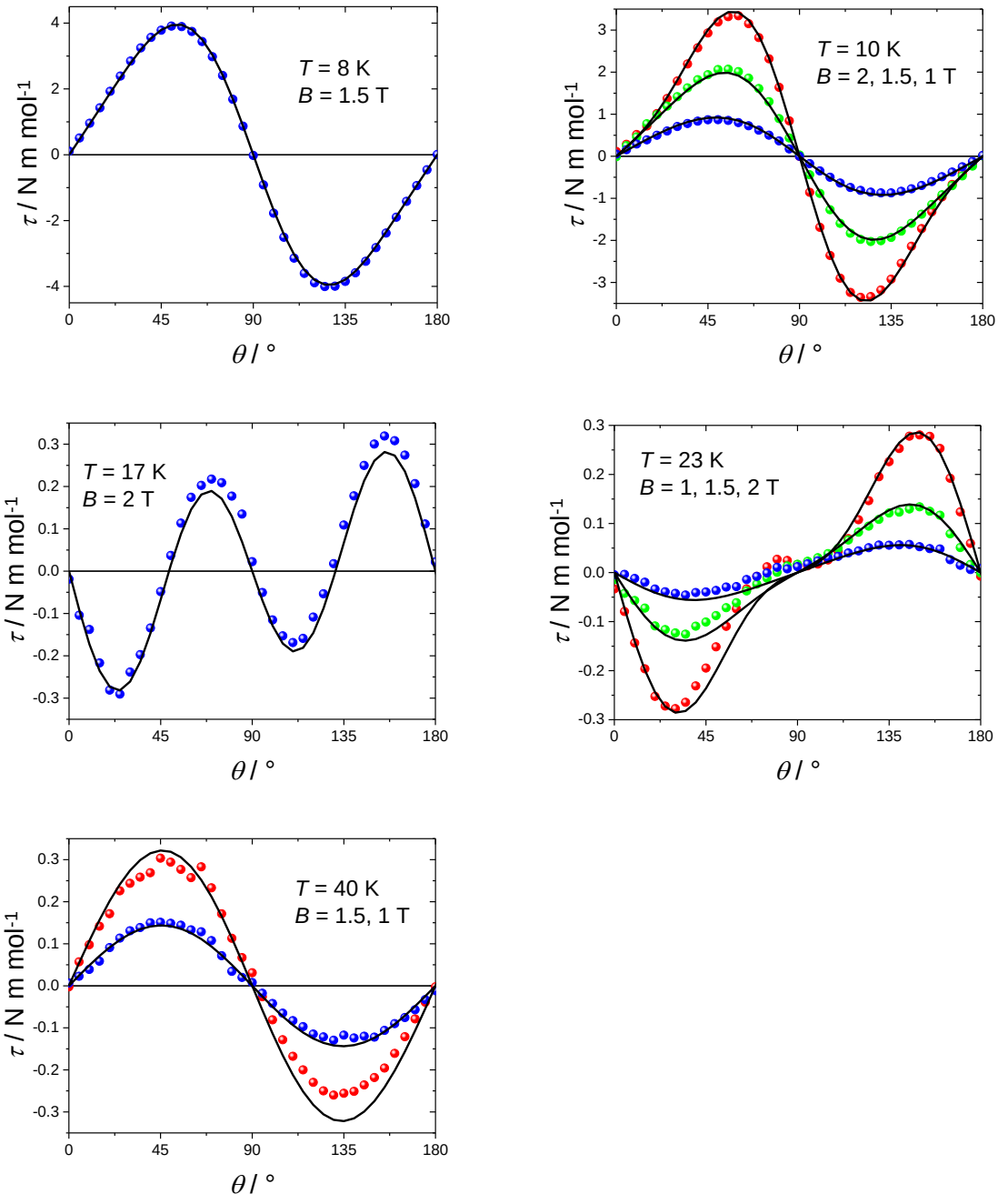

Figure S11 Cantilever torque magnetometry measurements on DyES at several temperatures and magnetic fields. Symbols are experimental points and lines are best fits. The CF parameters (Stevens' notation[6, 12]) that we extracted are: b_2^0 = -0.72(1) cm^{-1}, b_4^0 = 4.46(9) 10^{-3} cm^{-1}, b_6^0 = -7.15(5) 10^{-5} cm^{-1}, b_6^6 = 3.35(8) 10^{-4} cm^{-1}.

References:

1. M. Perfetti, M. A. Sørensen, U. B. Hansen, H. Bamberger, S. Lenz, P. P. Hallmen, T. Fennell, G. G. Simeoni, A. Arauzo, J. Bartolomé, E. Bartolomé, K. Lefmann, H. Weihe, J. van Slageren and J. Bendix, *Adv. Funct. Mater.*, 2018, **28**, 1801846.
2. B. M. Flanagan, P. V. Bernhardt, E. R. Krausz, S. R. Lüthi and M. J. Riley, *Inorg. Chem.*, 2002, **41**, 5024-5033.
3. E. Lucaccini, J. J. Baldoví, L. Chelazzi, A.-L. Barra, F. Grepioni, J.-P. Costes and L. Sorace, *Inorg. Chem.*, 2017, **56**, 4728-4738.
4. N. Ishikawa, M. Sugita, T. Okubo, N. Tanaka, T. Lino and Y. Kaizu, *Inorg. Chem.*, 2003, **42**, 2440-2446.
5. M. A. AlDamen, S. Cardona-Serra, J. M. Clemente-Juan, E. Coronado, A. Gaita-Arino, C. Marti-Gastaldo, F. Luis and O. Montero, *Inorg. Chem.*, 2009, **48**, 3467-3479.
6. S. Cardona-Serra, J. Clemente-Juan, E. Coronado, A. Gaita-Ariño, A. Camón, M. Evangelisti, F. Luis, M. Martínez-Pérez and J. Sesé, *J. Am. Chem. Soc.*, 2012, **134**, 14982-14990.
7. A. Abragam and B. Bleaney, *Electron Paramagnetic Resonance of Transition Ions*, Dover, New York, 1986.
8. B. Judd, *Physical Review*, 1957, **127**, 750-755.
9. S. Hüfner, *Zeitschrift für Physik A Hadrons and nuclei*, 1962, **169**, 417-426.
10. E. H. Erath, *The Journal of chemical physics*, 1961, **34**, 1985-1989.
11. M. Perfetti, *Coord. Chem. Rev.*, 2017, **348**, 171-186.
12. K. W. H. Stevens, *Proceedings of the Physical Society A*, 1952, **65**, 209.